

### Monoliths of Aligned Silica-Polypeptide Hexagonal Platelets

Enrico G. Bellomo<sup>†</sup> and Timothy J. Deming<sup>\*‡</sup>

Contribution from the Materials Department, University of California, Santa Barbara, Santa Barbara, California 93106, and Bioengineering Department, University of California, Los Angeles, Los Angeles, California 90049

Received September 9, 2005; E-mail: demingt@seas.ucla.edu

**Abstract:** Water soluble  $\alpha$ -helical polypeptides were used to prepare silica coated hexagonal single crystal platelets in concentrated solutions. To our knowledge, there is no other instance where polymer single crystals, typically formed under high dilution, can be grown in a bulk material. This unprecedented self-assembly process relies on complex cooperative interactions where silica condensation mediates the growth of polypeptide crystals, which in turn template silica overgrowth. The helices were also used to align samples giving monoliths composed of highly oriented layers of platelets. Overall, this procedure allows preparation of composites with good structural order and complexity via a simple biomimetic process.

#### Introduction

Many recent reports have described biomimetic approaches for the synthesis of inorganic materials with intricate shapes.<sup>1</sup> A major goal of this work is the ability to replicate the complex morphologies found in natural minerals, such as the layered crystalline calcium carbonate tablets in abalone shells,<sup>2</sup> and the hierarchical patterns of amorphous silica in diatoms.<sup>3</sup> The ability to realize such structures in synthetic materials holds tremendous technological potential for applications in separations and lightweight structural composites,<sup>4</sup> as well as catalysis and sensing when the inorganic materials can be selectively functionalized.<sup>5</sup> Many early biomimetic approaches yielded only materials with high symmetry, such as spheres, cylinders and sheets that, although well-ordered on mesoscopic and nanoscopic scales, lacked the complexity of natural materials.<sup>6–8</sup> Recent efforts have focused heavily on the use of polycations, peptides, proteins, and polypeptides in effort to form more complex shapes.<sup>3,9–15</sup> The simplest of these systems utilize cationic

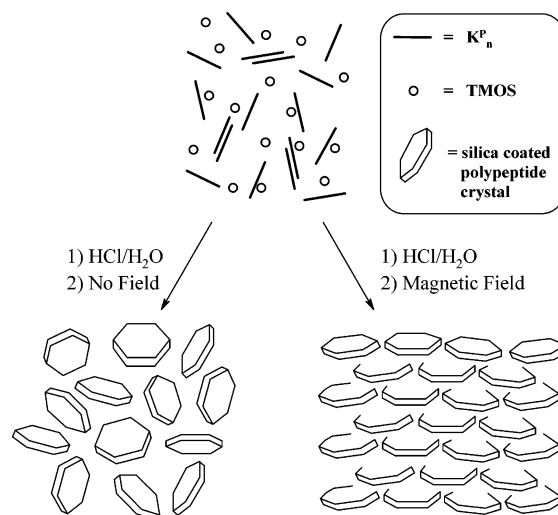


**Figure 1.** Schematic illustrating synthesis of silica-polypeptide crystal composites. Samples with macroscopic orientation were obtained by synthesis in the presence of a magnetic field.  $KP_n$  = rodlike, nonionic water soluble polypeptide (see Figure 2a). TMOS = tetramethyl orthosilicate. Drawings are not to scale.

polylysine, which can be used to organize amorphous silica into hexagonal platelets, spheres, and other shapes, although only under dilute conditions.<sup>16</sup> Here, we report formation of monoliths composed of silica-polypeptide composite hexagonal platelets utilizing a nonionic,  $\alpha$ -helical polypeptide in concentrated solutions (Figure 1). The high polypeptide concentration also allowed alignment of the platelets normal to an applied magnetic field, yielding long-range order in the monoliths. This one-pot assembly process demonstrates cooperativity between the silica precursors and the helical polypeptides, where the silica directs unprecedented formation of polypeptide single crystals at high concentrations, and the resulting crystals then act as templates for silica condensation. The resulting composites are the first

<sup>†</sup> Materials Department, University of California, Santa Barbara.

<sup>‡</sup> Bioengineering Department, University of California, Los Angeles.

- (1) Aizenberg, J. *Adv. Mater.* **2004**, *16*, 1295–1302.
- (2) Belcher, A. M.; Christensen, R. J.; Hansma, P. K.; Stucky, G. D.; Morse, D. E. *Nature* **1996**, *381*, 56–58.
- (3) Morse, D. E. *Trends Biotechnol.* **1999**, *17*, 230–232.
- (4) Davis, M. E. *Nature* **2002**, *417*, 813–821.
- (5) Bartl, M. H.; Boettcher, S. W.; Frindell, K. L.; Stucky, G. D. *Acc. Chem. Res.* **2005**, *38*, 263–271.
- (6) Attard, G. S.; Glyde, J. C.; Göltner, C. G. *Nature* **1995**, *378*, 366–368.
- (7) Tolbert, S. H.; Firouzi, A.; Stucky, G. D.; Chmelka, B. F. *Science* **1997**, *278*, 264–268.
- (8) Göltner, C. G.; Henke, S.; Weissenberger, M. C.; Antonietti, M. *Angew. Chem., Int. Ed. Engl.* **1998**, *37*, 613–616.
- (9) Kröger, N.; Lehmann, G.; Rachel, R.; Stumper, M. *Eur. J. Biochem.* **1997**, *250*, 99–105.
- (10) Naik, R. R.; Whitlock, P. W.; Rodriguez, F.; Brott, L. L.; Glawe, D. D.; Clarson, S. J.; Stone, M. O. *Chem. Commun.* **2003**, 238–239.
- (11) Patwardhan, S. V.; Mukherjee, N.; Steinitz-Kannan, M.; Clarson, S. J. *Chem. Commun.* **2003**, 1122–1123.
- (12) Cha, J. N.; Stucky, G. D.; Morse, D. E.; Deming, T. J. *Nature* **2000**, *403*, 289–292.
- (13) Hawkins, K. M.; Wang, S. S–S.; Ford, D. M.; Shantz, D. F. *J. Am. Chem. Soc.* **2004**, *126*, 9112–9119.
- (14) Jin, R.-H.; Yuan, J.-J. *Chem. Commun.* **2005**, 1399–1401.
- (15) Yuan, J.-J.; Jin, R.-H. *Adv. Materials* **2005**, *17*, 885–888.

- (16) Rodriguez, F.; Glawe, D. D.; Naik, R. R.; Hallinan, K. P.; Stone, M. O. *Biomacromolecules* **2004**, *5*, 261–265.

example where amorphous silica is organized into macroscopically oriented monoliths composed of layered crystal shaped platelets, demonstrating that complex architectures can be readily obtained from simple precursors.

## Discussion

In polylysine mediated silica synthesis, the water-soluble polypeptide chains are initially in a disordered configuration due to electrostatic repulsions between the like-charged ammonium side-chains.<sup>16</sup> Upon complexation with multivalent counterions, these chains can adopt ordered conformations (i.e.,  $\beta$ -sheet and  $\alpha$ -helix) that are able to crystallize. In the presence of silicic acid at neutral pH, cationic polylysine interacts with silicate anions to form helical chains that further condense to form composites. In dilute mixtures, hexagonal polylysine single-crystal platelets are formed that become coated with silica and settle out of the medium as a precipitate.<sup>17</sup> This technique can also be used to form silica composite platelets on anionic substrates, such as ITO glass, for sensing applications.<sup>18</sup> An important consideration in this system is that single platelets only form under highly dilute conditions (<1 wt% polylysine),<sup>17</sup> where formation of polypeptide single crystals is favored by slow, controlled crystal growth.<sup>19</sup> Virtually all polymeric single crystals are formed at high dilution for similar reasons: polycrystalline aggregates and semicrystalline structures will form at higher concentrations where interchain interactions are elevated.<sup>20</sup> The need to use high dilution to form hexagonally patterned silica composites precludes the formation of monoliths that may be useful in separations or structural applications.

To form solid composites, we recognized the advantage of performing synthesis at high concentrations of both silica precursor and polypeptide. Landmark studies utilizing lyotropic liquid crystal phases of surfactants or amphiphilic block copolymers to organize mesoporous silica structures provided the guidelines for preparation of polypeptide-silica monoliths.<sup>6–8</sup> However, the strong interaction between highly charged polylysine and silica precursors prevents use of this polypeptide at high concentrations since the rapidity of condensation and coprecipitation prevents formation of well-ordered materials.<sup>16</sup> Consequently, ethylene glycol-modified lysine building blocks were utilized to prepare water soluble, nonionic polypeptides,  $K^P_n$  ( $n$  = number of residues, Figure 2a),<sup>21</sup> that were expected to interact with silica precursors in a manner similar to the poly-(ethylene glycol) segments of pluronic block copolymers, used extensively to form ordered silica composites.<sup>6–8</sup>

An added feature of the  $K^P_n$  polypeptides is that they adopt very stable  $\alpha$ -helical conformations, and these rodlike molecules are capable of forming lyotropic liquid crystalline (LC) phases (cholesteric and hexagonal) at high concentrations in aqueous solution.<sup>22</sup> Initially, we envisioned mixing a silica precursor (e.g., tetramethyl orthosilicate, TMOS) and a catalyst (e.g., HCl) with highly concentrated solutions of  $K^P_n$  to form mixtures where the polypeptide LC would serve as a template for the inorganic

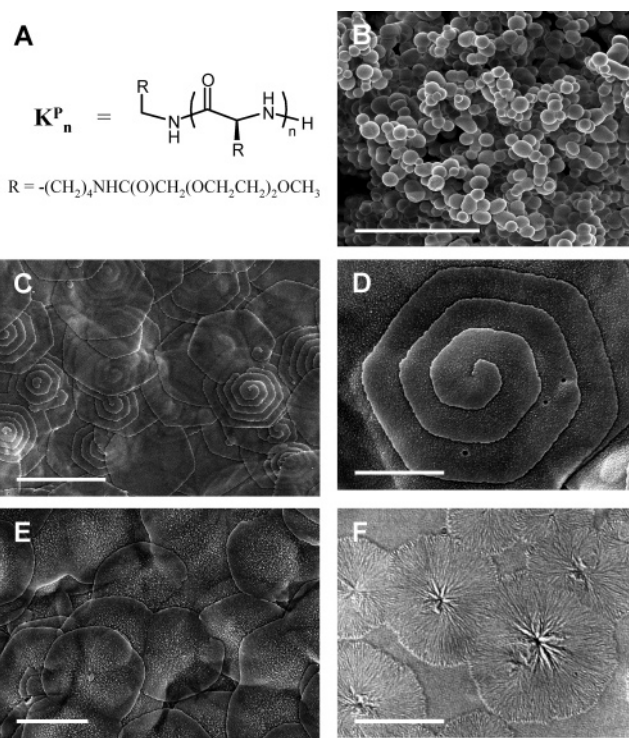


**Figure 2.** Morphologies of silica- $K^P_n$  polypeptide composites and  $K^P_n$  homopolymer. (A) Chemical structure of  $K^P_n$ . (B) SEM image of silica- $K^P_{56}$  (40 wt.% polypeptide) composite spheres (Bar = 50  $\mu\text{m}$ ). (C) SEM top view image of silica- $K^P_{264}$  (85 wt. % polypeptide) composite hexagonal plates (Bar = 10  $\mu\text{m}$ ). (D) Close up SEM image of a silica- $K^P_{264}$  (65 wt. % polypeptide) composite hexagonal plate (Bar = 2  $\mu\text{m}$ ). (E) SEM top view image of silica- $K^P_{400}$  (55 wt. % polypeptide, 1:1 mixture of D- and L-polypeptides) composite hexagonal plates (Bar = 2  $\mu\text{m}$ ). (F) Optical microscopy image of  $K^P_{300}$  spherulites grown by evaporation from a TFA/water solution (Bar = 50  $\mu\text{m}$ ).

phase. We were especially interested to see if the silica would penetrate the LC, where the rod-rod spacing of the polypeptide chains should increase with increasing volume fractions of silica. In any event, we reasoned that the interactions between intermediate silica species and the nonionic  $K^P_n$  chains should be relatively weak, allowing the self-assembling molecules to anneal into well-ordered structures, even under highly concentrated conditions.

## Results

When neat TMOS was added to LC solutions of  $K^P_n$ , the high viscosity of the LC phase prevented good mixing and only macroscopically phase separated mixtures of silica and polymer were obtained after hydrolysis. Consequently, composites were prepared using less concentrated, non-LC solutions of  $K^P_n$  (ca. 10 wt%), which were mixed with neat TMOS and aqueous HCl to bring the overall mixture to pH 3 for catalysis of silica formation.<sup>23</sup> The relative amounts of  $K^P_n$  and TMOS were varied to give composites where the final weight fraction of polypeptide ranged from 25 to 85% after drying. The degree of polymerization of the  $K^P_n$  chains was also varied from an average of 56 to 530 to evaluate the role of chain length in composite formation. Since chain length strongly affects the concentration of the isotropic to LC phase transition for  $K^P_n$  in water,<sup>22</sup> significant changes in composite structure with polypeptide chain length were expected. For all mixtures, samples were

(17) Tomczak, M. M.; Glawe, D. D.; Drummy, L. F.; Lawrence, C. G.; Stone, M. O.; Perry, C. C.; Pochan, D. J.; Deming, T. J.; Naik, R. R. *J. Am. Chem. Soc.* **2005**, *127*, 12577–12582.

(18) Glawe, D. D.; Rodriguez, F.; Stone, M. O.; Naik, R. R. *Langmuir* **2005**, *21*, 717–720.

(19) Cui, H.; Krikorian, V.; Thompson, J.; Nowak, A. P.; Deming, T. J.; Pochan, D. J. *Macromolecules* **2005**, *38*, 7371–7377.

(20) P. H. Geil *Polymer Single Crystals*; John Wiley and Sons: New York, 1963.

(21) Yu, M.; Nowak, A. P.; Pochan, D. P.; Deming, T. J. *J. Am. Chem. Soc.* **1999**, *121*, 12210–12211.

(22) Bellomo, E. G.; Davidson, P.; Impéror-Clerc, M.; Deming, T. J. *J. Am. Chem. Soc.* **2004**, *126*, 9101–9105.

(23) Devreux, F.; Boilot, J. P.; Chaput, F.; Leconte, A. *Phys. Rev. A* **1990**, *41*, 6901–6909.

thoroughly mixed and the initially clear solutions were placed in 1.5 mm diameter quartz capillary tubes and allowed to react at ambient temperature. The samples became opaque within 30 min, and had formed solid gels after 48 h. The samples were then removed from the capillaries and dried in a vacuum oven at 20 °C to constant weight. Analysis of the samples using  $^{29}\text{Si}$  NMR showed the presence of  $\text{Q}^2$ ,  $\text{Q}^3$ , and  $\text{Q}^4$  species indicating that the samples are hydrated silica.

The composites prepared using the short chain polypeptide  $\text{K}^{\text{P}}_{56}$ , regardless of polymer content (25 to 57 wt.%), crumbled into powders after drying. However, samples prepared with polypeptides greater than 200 residues long were obtained as solid monoliths that retained the cylindrical shape of the capillaries even after shrinkage caused by drying. The samples were cleaved to reveal the interior structure, which was imaged using SEM. All samples with low weight fractions of polypeptide formed highly irregular morphologies, with the degree of regularity improving with increasing polymer weight fraction. At higher fractions of  $\text{K}^{\text{P}}_{56}$  (e.g., 40 wt.%), composites were obtained as uniform spherical particles approximately 5 to 10  $\mu\text{m}$  in diameter (Figure 2b). More importantly, composites prepared with greater than 40 wt.% of longer  $\text{K}^{\text{P}}_n$  chains were obtained as agglomerates of well-defined hexagonal platelets (Figure 2c).

Many of the platelets were unilamellar single crystals, however some were found to be multilamellar or contain a central screw dislocation (Figure 2d), similar to polylysine single crystals.<sup>24</sup> The screw dislocations could be suppressed by use of 1:1 mixtures of enantiomeric D- $\text{K}^{\text{P}}_n$  and L- $\text{K}^{\text{P}}_n$  helices, which gave only unilamellar platelets (Figure 2e). Composite formation using D/L-random copolymer  $\text{K}^{\text{P}}_n$  chains, which are not  $\alpha$ -helical,<sup>25</sup> or  $\text{K}^{\text{P}}_n$  chains with large chain length distributions (i.e.,  $M_w/M_n > 1.4$ ) resulted in disordered composites with no hexagonal platelets. In the absence of silica, a concentrated solution of  $\text{K}^{\text{P}}_{300}$  crystallized only as large polycrystalline spherulites upon evaporation (Figure 2f), showing the importance of polypeptide-silica interactions during assembly.

Sample compositions were determined by TGA analysis, where it was found that the polypeptide could be removed by calcination above 300 °C. The samples were found to contain little water (<3 wt. %) and polypeptide weight fractions were within 3% of predicted values. SEM images of calcined samples showed little change from those with polypeptide, indicating the hexagonal platelets contain enough silica to maintain their shape even after removal of the polypeptide (Figure 3a). Analysis of the samples by WAXS showed the silica to be amorphous since only a single diffraction peak was observed corresponding to the interhelical distance between packed polypeptide rods (Figure 4a). This spacing was found to be invariant with respect to silica content in the composites, and was identical to the spacing found for pure  $\text{K}^{\text{P}}_n$  in the bulk (ca. 2.4 nm).<sup>19</sup> This result indicated that polypeptide helices were closely packed and that little, if any, silica was present between the helices.

After calcination, the diffraction peak disappeared, confirming that it was due to polypeptide and that the silica was amorphous. Although well-ordered hexagonal platelets were observable by SEM, no higher order diffraction peaks were seen by WAXS due to the instrument configuration. To determine if the helices were packed with long range order, individual platelets were

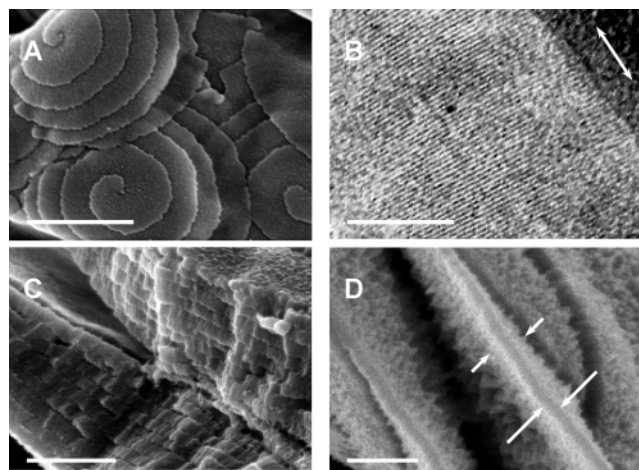


**Figure 3.** Images of silica- $\text{K}^{\text{P}}_n$  polypeptide composite structure. (A) SEM image of silica- $\text{K}^{\text{P}}_{300}$  (50 wt.% polypeptide) composite hexagonal plates after removal of polymer by calcination (Bar = 2  $\mu\text{m}$ ). (B) TEM image of a 200-nm thick cross-section of a silica- $\text{K}^{\text{P}}_{530}$  (46 wt. % polypeptide) composite plate. Arrows show orientation of plate surface (Bar = 50 nm). (C) SEM image of silica- $\text{K}^{\text{P}}_{250}$  (55 wt.% polypeptide) composite hexagonal plate cross sections after fracture showing multilamellar structure (Bar = 500 nm). (D) SEM image of silica- $\text{K}^{\text{P}}_{530}$  (65 wt. % polypeptide) composite hexagonal plate cross sections with partial silica deposition. Large arrows indicate uniform band of polypeptide, small arrows indicate irregular silica coating (Bar = 200 nm).

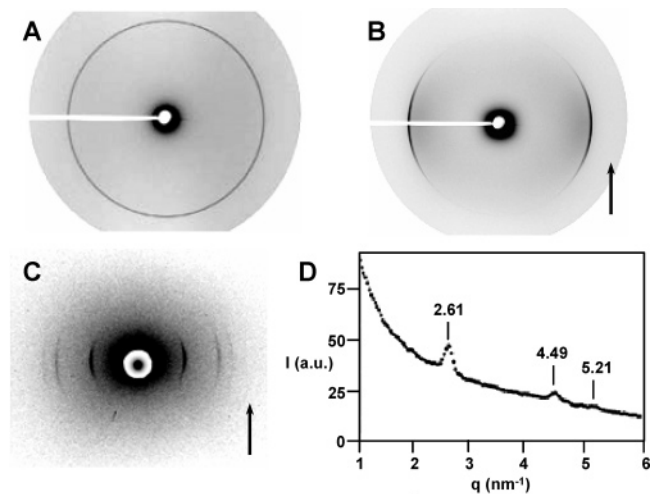


**Figure 4.** X-ray scattering data from silica- $\text{K}^{\text{P}}_n$  polypeptide composites. (A) Two-dimensional X-ray pattern from an unaligned silica- $\text{K}^{\text{P}}_{530}$  (43 wt.% polypeptide) composite ( $d$  spacing = 2.35 nm). (B) Two-dimensional X-ray pattern from a magnetic field (4.7 T) aligned silica- $\text{K}^{\text{P}}_{530}$  (43 wt.% polypeptide) composite ( $d$  spacing = 2.35 nm). Arrow indicates direction of applied magnetic field. (C and D) Wide-angle X-ray data of a magnetic field (4.7 T) aligned silica- $\text{K}^{\text{P}}_{530}$  (43 wt.% polypeptide) composite, loaded with 0.1 molar equiv. of  $\text{EuCl}_3$  per ethylene glycol side-chain, showing higher order reflections. (C) Two-dimensional X-ray pattern. Arrow indicates direction of applied magnetic field. (D) Radial  $I$  versus  $q$  X-ray scattering pattern showing hexagonal symmetry of the polypeptide lattice with diffraction lines in the ratio of 1,  $3^{1/2}$ , 2. Numbers indicate the peak values of  $q$ .

examined by TEM. A composite sample (46 wt. %  $\text{K}^{\text{P}}_{530}$ ) was impregnated with epoxy resin and then microtomed to give a 200 nm thick slice, which was imaged directly. Examination of the cross-section of a platelet showed a pattern of parallel lines ca. 2.3 nm apart running nearly perpendicular to the platelet surface (Figure 3b). These lines correspond to the individual rodlike polypeptide helices,<sup>17</sup> which show good long range order and alignment within a platelet.

(24) Padden, F. J.; Keith, H. D.; Giannoni, G. *Biopolymers* **1969**, *7*, 793–804.  
 (25) Bellomo, E. G.; Wyrsta, M. D.; Pakstis, L.; Pochan, D. J.; Deming, T. J. *Nat. Mater.* **2004**, *3*, 244–248.

All of these data suggest a model where the  $K^P_n$  chains assemble into hexagonal platelet crystals, which are then coated with silica to yield composites.<sup>17</sup> Some insights into the growth process were obtained by SEM of fractured samples. From cross sectional views, many of the platelets were found to be multilamellar, with individual platelets having thicknesses of ca. 80 to 120 nm, regardless of polymer length or concentration (Figure 3c). Since the lengths of the polypeptide chains were only 45 to 80 nm, and since the platelets remained intact after calcination, it was concluded that the extra thickness in each platelet was due to silica. This interpretation was substantiated by SEM images where cross-sections of crystals with partial silica coatings were observed revealing crystal layers of uniform width (ca. 35 nm) surrounded by irregular coatings of ca. 20 to 40 nm thickness (Figure 3d). Interestingly, since each platelet in a multilamellar stack was coated with a roughly even thickness of silica it implies that polypeptide crystallization and silica deposition occur concurrently. If this were not the case, then one would expect the multilamellar crystals to be coated with a thick layer of silica only on the outermost surfaces of the crystal stack. Coordinated polypeptide crystallization and silica deposition also explains the cooperativity that occurs between silica species and the polypeptides. Without silica, formation of single-crystal platelets does not occur at these polypeptide concentrations, indicating the inorganic species mediate the crystal growth process.

Formation of a large number of single crystals, as opposed to a smaller number of large polycrystalline spherulites, implies a high crystal nucleation rate and a slow controlled growth phase. The nonionic nature of the  $K^P_n$  chains as compared to cationic polylysine leads to a much weaker interaction between  $K^P_n$  and anionic silica species. However, the ethylene glycol side-chains of  $K^P_n$  can become partially protonated under the acidic synthesis conditions to give a slightly cationic polypeptide.<sup>21</sup> Alternatively, the ethylene glycol side-chains might hydrogen bond to silica species, or release bound water upon complexing to silica, in effect a hydrophobic interaction. It appears that during synthesis, some combination of these interactions is enough to associate an agglomerate of silica to a nucleus of polypeptide chains, which then grows into a crystal as the silica particles condense. The interaction between the  $K^P_n$  chains and silica must be robust enough to bring the chains together in water, which is a good solvent for  $K^P_n$ , yet must also be transient enough to allow annealing of the polypeptide chains into a highly ordered lattice. The balance of these interactions under our conditions appears to be near ideal since attempted syntheses in methanol or without an acid catalyst yielded a few hexagonal plates but mainly highly disordered composites. Overall, the stable  $\alpha$ -helical conformations of  $K^P_n$  chains, combined with their ethylene glycol side chains, were found to be critical features for formation of polypeptide single crystal composites under highly concentrated conditions.

The helical nature of the polypeptides also provides a means to modify macroscopic composite properties by alignment of the helices in electric or magnetic fields.<sup>26</sup> Since the helices are inherently aligned normal to the crystal platelets, alignment of the helices with a field should also yield long range ordering of the platelets themselves. In aqueous liquid crystals of  $K^P_n$ , we have shown that the rodlike helices can be well-aligned

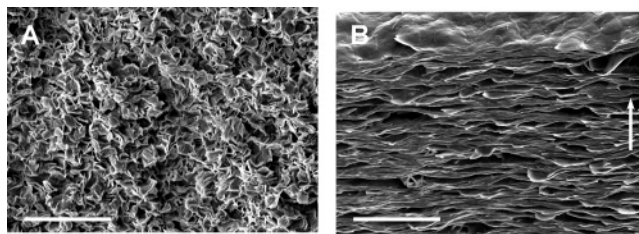


**Figure 5.** Images of silica- $K^{P400}$  (55 wt.% polypeptide, 1:1 mixture of D- and L-polypeptides) composite monoliths. (A) SEM image of unaligned monolith cross section after fracture showing disordered packing of hexagonal plates (Bar = 20  $\mu\text{m}$ ). (B) SEM image of magnetic field (4.7 T) aligned monolith cross section after fracture showing layering of hexagonal plates (Bar = 20  $\mu\text{m}$ ). Arrow indicates direction of applied magnetic field.

parallel to either a shear flow or an applied magnetic field.<sup>22</sup> Furthermore, addition of metal ions with high magnetic susceptibilities (e.g.,  $\text{Eu}^{3+}$ ) to  $K^P_n$ , which can bind to the ethyleneglycol side chains of the polypeptide, facilitates alignment of the helical chains under mild conditions.<sup>27</sup> When composite preparations were subjected to a 4.7 T magnetic field for 8 h immediately after mixing, composites were obtained with a high degree of helix orientation, as measured by WAXS (Figure 4a,b). Addition of 0.1 equiv of  $\text{EuCl}_3$  per ethylene glycol side-chain of  $K^P_n$  to composite preparations combined with alignment in a magnetic field gave rise to an even higher degree of orientation, detectable with a wider angle X-ray instrument (Figure 4c). The improved electron density contrast in these samples also allowed detection of higher order diffraction peaks in a ratio of 1 to  $3^{1/2}$  to 2 that confirmed the hexagonal ordering of helical chains in the crystals (Figure 4c,d).

The macroscopic orientation of these field-aligned composites was readily observed by SEM. Figure 5a is an unaligned sample where the random orientation of the platelets into a porous network is clearly visible. However, when the sample was prepared in a magnetic field (Figure 5b), the platelets align predominantly perpendicular to the applied field and consequently form a layered composite with highly anisotropic structural features. The ability to readily align the polypeptide helices, and thus control platelet orientation, provides a simple process to tailor the properties of these materials. Platelet orientation is expected to significantly affect the permeability of these materials in separations, and provides a means to prepare coatings and control presentation of surface functionality. This one-pot process to prepare composites of good structural order and complexity, which utilizes polypeptides of defined structure and functionality, is a promising methodology for biomimetic synthesis of composite materials.

**Acknowledgment.** This work was supported by the MRSEC program of the National Science Foundation under award No. DMR-0080034. E.G.B. would like to thank Ryan Hayward for discussions and assistance with the TEM images. The authors also thank Jarrod Hanson for the optical microscopy image of  $K^P_n$  spherulites.

**Supporting Information Available:** Details of all materials and measurements. This material is available free of charge via the Internet at <http://pubs.acs.org>.

JA056227H

(26) Panar, M.; Phillips, W. D. *J. Am. Chem. Soc.* **1968**, *90*, 3880–3882.

(27) Barmatov, E. B.; Pebalk, D. A.; Barmatova, M. V.; Shibaev, V. P. *Polymer* **2002**, *43*, 2875–2880.